

Nanoscale

Accepted Manuscript



This is an *Accepted Manuscript*, which has been through the Royal Society of Chemistry peer review process and has been accepted for publication.

Accepted Manuscripts are published online shortly after acceptance, before technical editing, formatting and proof reading. Using this free service, authors can make their results available to the community, in citable form, before we publish the edited article. We will replace this *Accepted Manuscript* with the edited and formatted *Advance Article* as soon as it is available.

You can find more information about *Accepted Manuscripts* in the [Information for Authors](#).

Please note that technical editing may introduce minor changes to the text and/or graphics, which may alter content. The journal's standard [Terms & Conditions](#) and the [Ethical guidelines](#) still apply. In no event shall the Royal Society of Chemistry be held responsible for any errors or omissions in this *Accepted Manuscript* or any consequences arising from the use of any information it contains.

ARTICLE

Cite this: DOI: 10.1039/x0xx00000x
3D plasmonic nanobowl platform for the study of exosomes in solution

Changwon Lee¹, Randy P. Carney², Sidhartha Hazari², Zachary Smith¹, Alisha Knudson², Christopher S. Robertson¹, Kit S. Lam^{1,2}, and Sebastian Wachsmann-Hogiu^{1,3*}

Received 00th January 2012,
Accepted 00th January 2012

DOI: 10.1039/x0xx00000x

www.rsc.org/

Thin silver film coated nanobowl Surface Enhanced Raman Spectroscopy (SERS) substrates are used to capture exosomes in solution for SERS measurements that can provide biochemical analysis of intact and ruptured exosomes. Exosomes derived via Total Exosome Isolation Reagent (TEIR) as well as ultracentrifugation (UC) from the SKOV3 cell line were analyzed. Spectra of exosomes derived via TEIR are dominated by a signal characteristic for the TEIR kit that needs to be subtracted for all measurements. Differences in SERS spectra recorded at different times during the drying of the exosome solution are statistically analyzed with Principal Component Analysis (PCA). At the beginning of the drying process, SERS spectra of exosomes exhibit peaks characteristic for both lipids and proteins. Later on during the drying process, new SERS peaks develop, suggesting that the initially intact exosome ruptures over time. This time-dependent evolution of SERS peaks enables analysis of exosomal membrane contents and the contents inside the exosomes.

Introduction

Exosomes are microvesicles in the size range of 30 to 100 nm formed inside of multivesicular bodies (MVBs) in the cell and released to extracellular space upon fusion of the MVBs and cellular membrane. Originally thought to function solely as a waste pathway, recent studies revealed that exosomes actually carry functional biological material and represent an important subset of microvesicular communication in the body. Exosomes are highly enriched in protein, signaling lipids, and genetic material, including mRNAs and miRNAs, all combining to mediate a vast amount of biological function. Proteins exist both membrane-bound and internally sequestered in the exosomes and are known to facilitate molecular targeting, anti-apoptosis, membrane fusion, antigenic peptide binding, signal transduction, T-cell stimulation and cytoskeleton arrangement¹. The relative abundance of exosomal protein, lipids, and genes vary with the composition and function of their parent cell, suggesting biological mechanisms in place for active sorting process during exosome production^{2,3}.

Especially intriguing in regards to disease diagnosis, exosomes secreted from abnormal cells (e.g. under stress, tumor cells, or otherwise affected) are typically secreted in variable number, and with a skewed distribution in composition. In recent studies, it was shown that exosomes also play a significant role in cancer metastasis through regulation of tumorigenic pathways, such as promoting angiogenesis in lung cancer ascites⁴, eliciting paracrine endothelial signaling pathway contributing metastatic process⁵, and affecting T-cells by inducing FAS ligand initiated apoptosis^{6,7}. Also, the relative abundance of miRNAs in tumor-driven exosomes compared to healthy cell-driven exosomes indicates that exosomes can be considered as probes of tumor formation⁸. As exosomes are found in

all body fluids including blood, urine and saliva⁹, they are currently considered as means for non-invasive cancer diagnostics¹⁰.

Out of the many, evolving methods to purify exosomes, two classes are the most common: (1) differential/gradient ultracentrifugation and (2) low-speed centrifugation commercial isolation kits. While commercial kits isolate roughly 100x greater number of exosomes¹¹, and are user-friendly, the agent itself acts by precipitating vesicles with polyethylene glycol or related polymers, resulting in contamination by non-exosome debris and the polymeric agent itself. In comparison, differential ultracentrifugation methodologies separate exosomes by size and/or buoyant density, leading to higher purification of the desired vesicle population, but remain highly tedious and not fit for high-throughput application. Furthermore, the lack of a unifying definition of what exactly constitutes an exosome has led to an uncertainty in choosing from the numerous protocols and commercial reagents reported to purify exosomes. For these reasons, we mainly focused on exosomes purified from a single commercial isolation kit due to consistently reproducible SERS measurement for those exosomes, and used ultracentrifuge-purified exosomes for comparison purposes.

The most common strategy for exosome analysis is the identification and classification of gene, protein and lipid compositions through extensive genomic, proteomic and lipidomic approaches¹²⁻¹⁴. Despite providing high-resolution molecular information of exosomal content, these methods require complicated, time-consuming protocols, and are extremely cost inefficient in regards to the amount of exosome generation required for a single measurement. Thus there are needs for simpler and faster methods to analyze molecular components of exosomes, such as optical technology. Although many optical methods have been used to analyze exosomes, most of them provide only limited biochemical information¹⁵. For example,

fluorophore assisted methods such as fluorescence microscopy (FM)¹⁶, fluorescence correlation microscopy (FCM)¹⁷, and stimulated emission depletion microscopy (SEDM)¹⁸ provide the biochemical information of only targeted biological components in the exosome and other scattering techniques such as dynamic light scattering (DLS)¹⁹, nanoparticle tracking analysis (NTA)²⁰, and scattering flow cytometry (SFC)²¹ only provide physical information such as size distribution of the exosomes.

To address these shortcomings associated with characterizing exosome content by current optical methods, we decided to employ Raman spectroscopy, an important analytical technique with the potential to provide information about the biochemical content of exosomes. In its simplest form, spontaneous Raman spectroscopy has been used in combination with laser trapping for the characterization of extracellular vesicles derived from *Dictyostelium discoideum* cells. This study revealed that the ratio between the lipids, DNA, and proteins changes for vesicles derived from cells in different physiological states.²² Yet laser-trapping is a single exosome measurement technique and therefore is extremely laborious, slow, and lacks surface specificity. Instead, Kerr et al.²³ reported Surface-enhanced Raman Spectroscopy (SERS) analysis on ovarian tumor derived exosomes by mixing the exosomes with gold nanoparticles, but quantitative SERS measurement using metallic nanoparticles has been long-plagued by background Raman signals from the nanoparticles' stabilizing surface ligands, and inconsistency of the SERS intensity arising from non-uniform hot-spot generation as a result of irregular aggregation of the nanoparticles during drying processes.

In this paper, we show that nanobowl-like plasmonic substrates can be used to capture and analyze exosomes for their chemical content via SERS measurements. The active surfaces are fabricated via soft lithography on flexible PDMS substrates on which a thin layer of silver is sputtered. Soft lithography is a fabrication method using elastomeric molds such as PDMS. This method is an alternative technique for photolithography and its common characteristic is the reliance on physical contact of the stamp with the substrate. The physical contact is the mediator of the resulting pattern and its resolution is limited only by van der Waals contact and atomic/molecular granularity. It has various advantages including low cost and simplicity compared to traditional photolithography methods. Soft lithography methods using colloidal particles have been studied previously for nanostructure fabrication²⁴⁻²⁷. These substrates have several unique advantages for the detection of small biological vesicles such as exosomes. First, due to the small size of the nanobowls, very few exosomes are captured and measured with a focused beam inside a single bowl, allowing analysis of a few exosomes at a time. Second, the exosomes are trapped inside the submicron-sized nanobowl and the signal is generated from a narrow volume near the plasmonic surface. Third, both intact and burst exosomes can be analyzed. In addition, the sputtered plasmonic surface has lower SERS background compared with SERS particles prepared via reduction methods.

Experimental

Materials

DCM (dichloromethane) and ethanol were purchased from Sigma (St. Louis, MO), PDMS (polydimethylsiloxane) elastomer kit was purchased from Dow Corning (Carrollton, KY). Sulfate latex polystyrene beads and Total Exosome Isolation Reagent 4478359 (TEIR, hereafter) were purchased from Life Technologies® (Grand Island, NY)

Fabrication of nanobowl structures on a PDMS template

To obtain PDMS nanobowl templates, a 10 μ L solution of 1 μ m sulfate latex polystyrene beads was dropped on a clean glass slide surface and dried in the oven (100 °C) for approximately 10 minutes. The dried spot is roughly 3–4 mm in diameter. Pre-mixed PDMS elastomer and initiator (10 to 1 ratio) was then poured gently on the dried latex beads layer on top of the glass slide and cured for 2 hours in the oven at 100 °C. After 2 hours, the hardened PDMS layer was peeled off from the glass slide and washed with DCM to remove any latex beads bound to the PDMS surface. Highly uniform hexagonal nanobowl structures with a lattice constant of 1.7 μ m, diameter of 800 nm and nanobowl depth of 300 nm were obtained in this way on the PDMS. The area outside the nanobowl region was flat PDMS. The size of the nanobowls was selected for the optimum SERS signal generation for the incident laser wavelength of 633 nm²⁴. The prepared PDMS templates were then sputtered with a 40 nm silver layer using a Kurt J. Lesker sputterer (Jefferson Hills, PA) at 10 mTorr and 300 mW.

Surface characterization

SEM was used for the structural characterization of the fabricated structures. All SEM images were obtained using a Hitachi S-4100T (Tokyo, Japan) instrument.

Exosome isolation and preparation

Exosomes were isolated from conditioned cell media. Briefly, SKOV3 cells are plated at ~25 % confluency in a T75 flask and incubated in appropriate growth medium supplemented with 10% FBS. After 24 hr, the media is replaced by one containing exosome-depleted FBS (bovine exosomes were removed from 30% FBS/media by ultracentrifugation at 100,000xg for 18 hr) in order to ensure that the resulting exosomes in the cell culture medium supernatant only originate from the plated cells. After 48 hr the cell culture media is harvested and centrifuged at 2,000xg for 30 min followed by 10,000xg for 40 min, to remove dead cells and cell debris/microvesicles, respectively. The exosome-containing supernatant is incubated with TEIR at 4 °C overnight during before final centrifugation at 10,000xg for 1 hr at 4 °C. The supernatant is aspirated to waste and the exosome-containing pellet is re-suspended in 100 μ L of 1XPBS for every 1 mL starting cell culture media volume. At this point, these exosomes are used *as is* for downstream analysis, and are stored at -20 °C until thawing to room temperature just prior to use. Western blot analysis was used to confirm the purity of the exosomal pellet. Exosomes were also extracted via differential ultracentrifugation, following previously reported methodology²⁸ and stored at -20 °C until use.

Exosome characterization

Western blot analysis to measure exosome protein content

The concentration of total exosome protein extract was determined by BCA assay. 30 μ g of cell lysate and 40 μ g of exosome protein were loaded per lane for SDS PAGE (polyacrylamide gel electrophoresis). After protein separation on the gel, the contents were transferred by gel electrophoresis and electroblotting. Blocking and washing the membrane before performing immunostaining against proteins enriched in exosomes was performed. As there are no exosome specific markers, a combination of proteins that are enriched in exosomes from all different cellular origins are commonly used for confirmation of exosome collection and purity. We confirmed the exosomes for containing tetraspanins (e.g. CD9, CD63) and proteins involved in multivesicular biogenesis (Tsg101

and alix), along with the negative control Calnexin (not found in exosomes). This data is presented in **Figure 1A**.

Nanoparticle Tracking Analysis (NTA)

NTA was run on the NanoSight LM10 equipped with a perfusion pump. Directly before NTA analysis, concentrated exosome samples were thawed from storage and diluted at least 1000x in freshly filtered PBS (using a 0.01 μm syringe filter; solution confirmed on the NTA to be free of nanoparticle contamination). Diluted exosome solutions were passed thrice through 0.2 μm Nylon syringe filters and immediately injected into the NTA at room temperature. Presented data represents the average and standard deviation of three consecutive measurements of the same sample. Each repetition recorded 1 minute of data, chosen so that at least 200 particle tracks were analyzed per video, with 30 sec of flow between measurements.

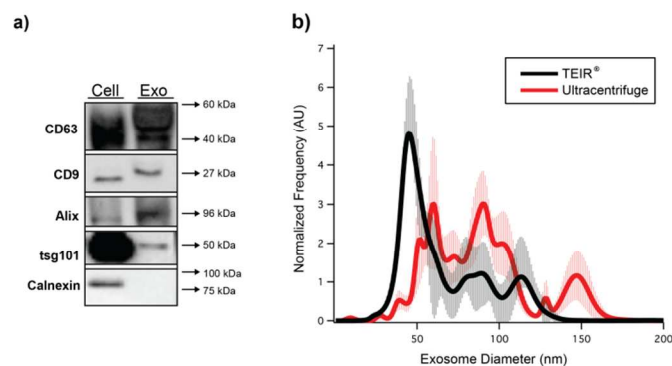


Figure 1: (a) Western Blot Characterization of SKOV3 cells and exosomes isolated via TEIR. SKOV3 total cell lysate and exosomal protein lysates (40 μg per lane) were compared by Western blot using several antibody markers both specific and nonspecific for exosomes. CD63 and CD9 are both markers for extracellular vesicles (including exosomes and ectosomes), while tsg101 and Alix are ESCRT-related proteins specific for MVB formation (exosomes only). The molecular weight for each protein is indicated on the right side of the figure. (B) NTA size analysis of exosomes.

SERS measurements

Exosomes were diluted using PBS buffer from the purified stock solution after the series of SERS measurements at different concentrations to determine the optimum concentration for the most consistent SERS measurement. This was done by diluting the exosome solution, and sampling the SERS signal in approximately 10-20 different spatial locations (corresponding to different nanobowls). The exosome concentration for best signal reproducibility corresponds to approximately 580 fM. For each sample, 20 μL of the diluted exosome solution was then dropped onto the SERS substrates and air-dried until the apparent liquid solution disappeared, resulting in exosomes captured in the nanobowls. At this point we believe the exosomes remain intact in solution due to the fact that the evaporation of the solution within the nanobowls has slowed significantly by increased surface tension. SERS was then measured using a Renishaw InVia Raman microscope (Gloucestershire, UK) with excitation wavelength at 633 nm and a 50X, 0.75NA objective lens that determines a spot size of approximately 1.25 micrometers. The exposure time was 10 s and laser power (measured after the objective) was 42 μW . For the time-dependent study, the same sample has been measured over the time period of 0 hr, 1 hr and 3 hr after the sample solution on the nanobowl substrate was apparently dried. The measurements were

performed on 10-20 different arbitrarily chosen spots of the substrate, and averaged for data presentation unless described otherwise. The background SERS spectrum of the TEIR kit solution was taken by drying the TEIR solution on the nanobowl substrate. The TEIR solution is very viscous and did not dry completely as it eventually forms a hydrogel-like structure on top of nanobowl substrate indicating its polymeric contents. Therefore the SERS spectra were taken after trapping the gel between the nanobowl substrate and glass cover slip.

FEM simulations

The uniformity of the SERS enhancement of the nanobowl array is demonstrated by FEM simulations using the COMSOL Multiphysics software package. Perfectly matched layers (PML) boundary conditions were used to terminate the simulation area. Meshing elements size was restricted to one tenth the wavelength. Using parameters similar to those in the experiment (633 nm excitation, beam size of 1.25 μm , focal plane x-axis, nanobowls with 800 nm diameter and 300 nm depth), and literature values for the permittivity of air ($\epsilon_r = 1.00058986$), PDMS ($\epsilon_r = 2.2776$), and silver, ($\epsilon_r = -16-0.5i$), field distributions were obtained for excitation in the center of the bowl and in between bowls, as seen in **Figure 2**. Comparison of the two cases indicates that the electric field distribution within a single bowl does not depend significantly on the position of the excitation beam with respect to the bowl.

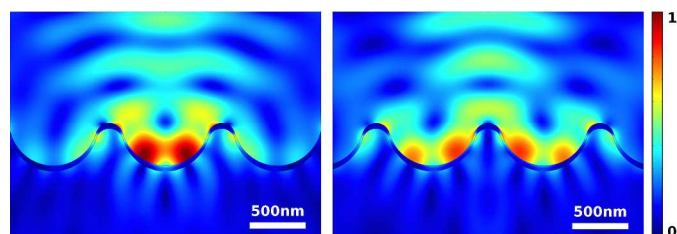


Figure 2: Near field surface plot of the electric field norm ($E = (|E_x|^2 + |E_y|^2)^{1/2}$) with Gaussian illumination at different incident laser beam position (left is centered on the bowl, right is centered between bowls). Both the excitation and scattered fields are shown in these figures.

Results and Discussion

Highly sensitive and reproducible silver thin-film coated, metallic nanobowl-structured SERS substrates were previously developed in our group^{24,29}. These unique nanobowl structures provide the ideal geometry for trapping nano-sized vesicles, such as exosomes, for SERS measurement, as the entire vesicle can be positioned within the SERS-active metallic nanobowl, as illustrated in **Figure 3**. On the other hand, **Figure 2** demonstrates that exosomes trapped inside the bowls are exposed to a relatively similar density of “hot-spots” regardless of the position of the excitation beam with respect to the bowl. Thus, unlike nanoparticle-based SERS substrates, where the randomly aggregated nanoparticles create significant variability in hot spot strengths, and the positioning of the analyte relative to hot spots³⁰, the nanobowl-structured substrates provide more reproducible SERS intensities that are more suitable for quantitative analysis of small analytes. While this aspect has been explored in a different article²⁹, here we focus on the spectral characterization of exosomes. An additional advantage of using the nanobowls for exosome analysis is the possibility of measuring only surface of the exosomes (which would contain the lipid bilayer and surface ligand proteins) instead of the entire contents of the exosomes, since the

SERS active volume exists mainly within ~ 5 nm distance from the nanobowl surface³¹, roughly the thickness of a lipid membrane.

As the water is dropped on the nanobowl substrate, the water will spread similarly to the “petal effect”, without trapping air in the nanostructure³². As a result of the “petal effect”, when water evaporates, the contact area between the water droplet and nanobowl structure does not change and only the height of the water droplet decreases. This process continues until a very thin film of water exists, which pushes the exosomes closer to the metal inside the nanobowls.

Even after apparent air drying, the submicron-sized nanobowls may contain residual water due to limited exposure to air of the solution contained in the very small curvature of a nanobowl. Thus, we hypothesize that at this stage the exosomes could maintain their intact form during the early time points of SERS measurement. Furthermore, despite the slowing evaporation rate as a result of increased surface tension in the nanobowl, eventually (\sim hours) the residual water evaporates enough such that the exosomes should burst under tension, and release their internal contents to the SERS active nanobowl surface. This process would result in a distinctive time-dependent SERS analysis of exosomal contents capable of resolving differences between surface and internal exosomal contents as illustrated in **Figure 3**.

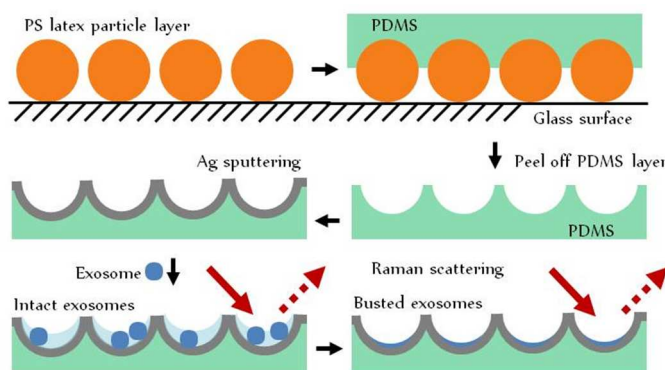


Figure 3: Schematic diagram of the silver film coated nanobowl substrate preparation and its use in SERS analysis of exosome both intact and ruptured forms.

As a proof-of-concept test and in order to demonstrate the relative physical dimensions of the nanobowls and exosomes, exosome-sized polystyrene beads (100 nm) were deposited and trapped inside the nanobowl substrates and analyzed by scanning electron microscopy (SEM) (**Figure 4**). Polystyrene beads were used for electron microscopic analysis because exosomes would easily burst under the electron beam. The polystyrene beads were indeed trapped inside the bowl and no polystyrene beads were found outside (on top) of the nanobowl structures, suggesting that the exosome-sized particles could be efficiently trapped inside the nanobowls.

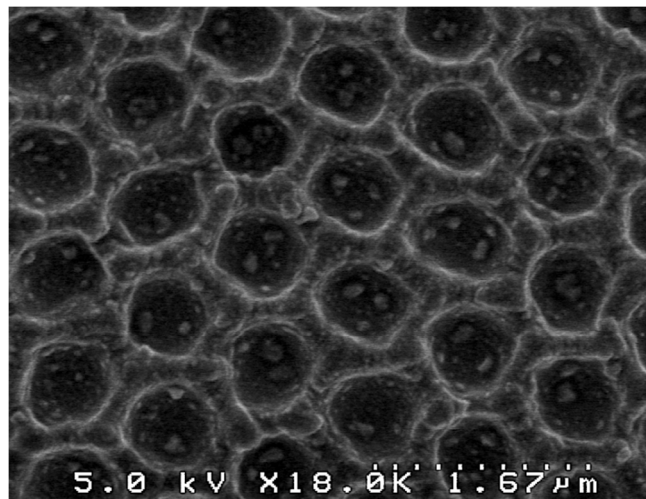


Figure 4: SEM image of a nanobowl substrate with 100 nm sized polystyrene beads trapped inside bowls. Note that the polystyrene beads are additionally coated with gold after deposition on the substrate. This step is necessary for SEM imaging.

The purified exosomes have initial concentrations of 291 pM for UC and 249 pM for TEIR as determined from NTA measurements. These exosomes were further diluted in the range of 78 fM to 580 fM to determine the most reproducible SERS measurements. The concentration used in this study was chosen for best reproducibility, which corresponds to approximately 1 exosome per nanobowl, or approximately 580 fM. This corresponds to a sensitivity that is approximately 10^3 -fold lower than that reported in a recent Surface Plasmon Resonance (SPR)-based study, and about 10-fold lower than the sensitivity of a chemiluminescence ELISA assay reported in the same study³³. However, as we can identify 1 exosome at a time in 1 nanobowl, our ultimate limit of detection should be limited only by the area scanned.

Our first observation indicated that exosomes purified via the commercial Total Exosome Isolation Reagent® (TEIR) kit showed a definitive set of peaks at early time points (**Figure 5A**, 0 hr spectra), matching closely the background SERS spectrum of the blank TEIR reagent itself (Raman peaks at 855, 1048, 1134, 1307 and 1473 cm^{-1} , **Figure 5A**). This indicates a strong affinity of the TEIR kit contents to the surface of exosomes, something entirely unexpected since the claimed function of the commercial precipitation reagents is to precipitate exosomes, *but not to adhere or bind them*.

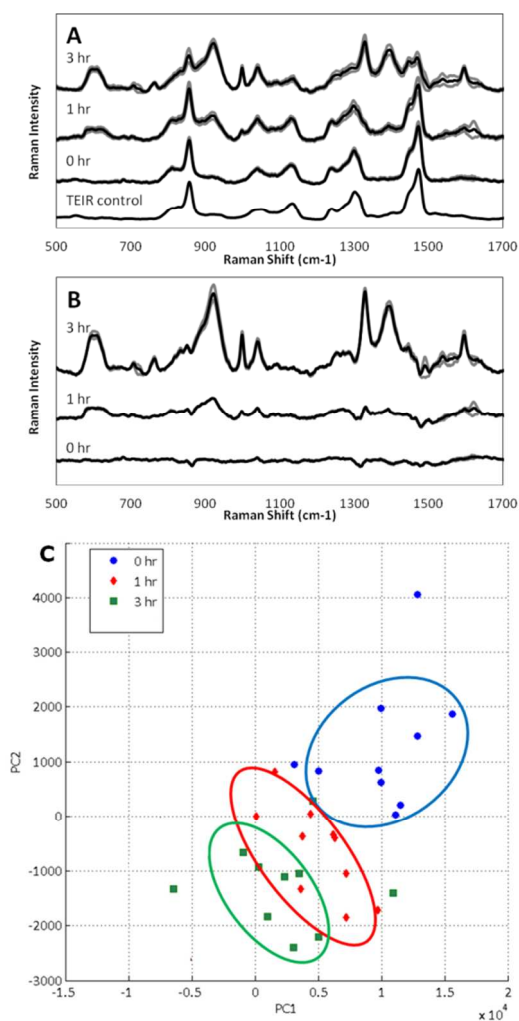


Figure 5: Timed SERS spectra of exosomes derived from SKOV3 cell line; (A) Comparison of the timed exosome SERS spectra with TEIR control, (B) Timed exosome SERS spectra after subtracting TEIR control spectra background. (Black lines: averaged spectra of each condition, grey lines: standard deviation), and (C) Principal Component Analysis of timed SERS spectra of exosomes derived from SKOV3 via TEIR.

In fact, in a previous report in the literature, the SERS peaks we measured as originating from the TEIR itself were mis-reported as exosome peaks³⁴. In that study, the authors used ExoQuick Exosome Precipitation Solution (System Biosciences, Mountain View, CA) which is different from the isolation kit that we used in this study but showed nearly identical SERS peaks. The strong presence of peaks originating from the isolation kit must be accounted for in future SERS studies employing this purification method.

In **Figure 5A**, it is clearly shown that the spectrum of the TEIR solution is present in the SERS spectra at all time points. At time 0 hr, defined as the moment the surface of the nanobowl area has been dried, the SERS spectra of exosome only show the peaks from TEIR. Since SERS is only sensitive to chemical components in the nearby vicinity (~5nm) of the substrate, this observation indicates that the outer surface of the exosome is completely surrounded by the compound found in the TEIR solution, apparently forming a polymeric layer with a thickness of at least 5 nm. Over the duration of the measurement, as the nanobowls continue to dry out, many

more peaks appeared, which can be visualized by blanking the TEIR solution observed from time 0 (**Figure 5B**, 3 hour spectra).

The major peaks which appeared over time are located at 615 (s, br, C-C twist protein) cm⁻¹, 645 (w, C-C twist Tyr) cm⁻¹, 707 (w, aminoacid methionine) cm⁻¹, 760 (m, Trp) cm⁻¹, 830 (m, Tyr) cm⁻¹, 920 (s, protein) cm⁻¹, 1000 (s, Phe) cm⁻¹, 1050 (m, lipid) cm⁻¹, 1120 (w, NA) cm⁻¹, 1175 (m, Tyr, Phe) cm⁻¹, 1211 (s, protein) cm⁻¹, 1330 (s, phospholipid) cm⁻¹, 1394 (s, NA) cm⁻¹, 1440 (s, lipid) cm⁻¹, 1552 (w, Trp) cm⁻¹, and 1600 (w, Phe) cm⁻¹. (Acronyms: s=strong, m=medium, w=weak, br=broad, NA=nucleic acid) As the peak assignment shows, newly appeared peaks are mostly typical for proteins, nucleic acids and lipids, which are main components of exosomes. We hypothesize that upon bursting, the exosomal contents are freed from sequestration by the TEIR agent in order to interact with the nanobowl surface and contribute to SERS signal. As an effort to statistically measure the differences between the timed spectra shown in Figure 4, Principal Component Analysis (PCA) was performed for 10 individual spectra at each time point (**Figure 5C**). The spectra cluster along the PC1 and PC2 axes into different groups specific for the time points at which the spectra were recorded.

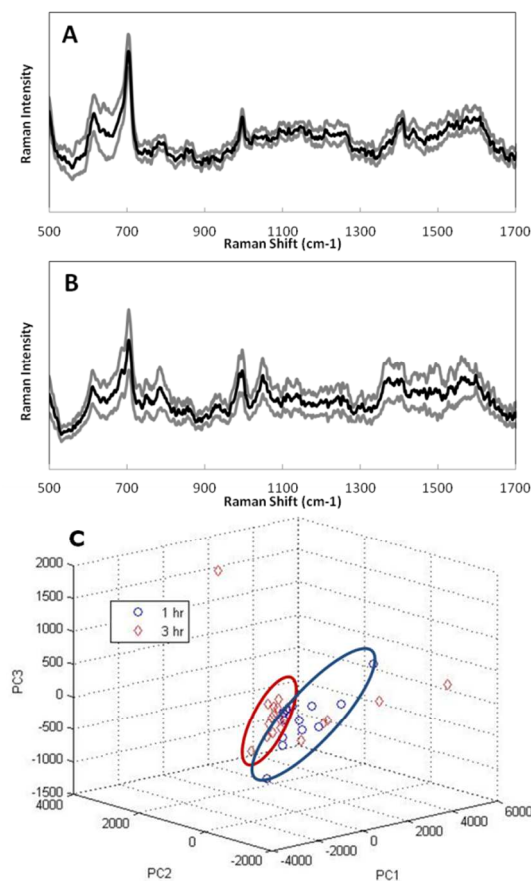


Figure 6: The SERS spectra of SKOV3 derived exosomes with UC purification method. (Black line: averaged spectrum, grey lines: standard deviation). (A) average of spectra recorded at 1 hour, (B) average of spectra recorded approximately 3 hours after apparent evaporation, and (C) principal component analysis of the SERS spectra taken at 1 hour and 3 hour time point.

In order to confirm that the emergence of the time dependent exosome peaks accompanying nanobowl drying is due to the hypothesized TEIR binding phenomenon, we compared the SERS experiment with exosomes purified by ultracentrifugation (Figure 6). The averaged SERS spectra (black lines) illustrate a consistency over time in these samples, instead of an emergence of peaks as observed in the TEIR purified exosome samples from the same SKOV-3 cells. Many of the peaks from UC purified exosomes are identical to the TEIR purified exosomes, while some are simply altered in intensity (such as the peak at 1000 cm^{-1} in both spectrum), and still others are wholly unique. The new peaks are located at $615\text{ (s, C-C twist protein)}\text{ cm}^{-1}$, $645\text{ (w, C-C twist Tyr)}\text{ cm}^{-1}$, $707\text{ (s, amino acid methionine)}\text{ cm}^{-1}$, $752\text{ (s, NA)}\text{ cm}^{-1}$, $786\text{ (m, NA)}\text{ cm}^{-1}$, $830\text{ (w, Tyr)}\text{ cm}^{-1}$, $852\text{ (w, Tyr)}\text{ cm}^{-1}$, $879\text{ (w, Trp)}\text{ cm}^{-1}$, $920\text{ (w, protein)}\text{ cm}^{-1}$, $937\text{ (w, protein backbone)}\text{ cm}^{-1}$, $1000\text{ (s, Phe)}\text{ cm}^{-1}$, $1050\text{ (m, lipid)}\text{ cm}^{-1}$, $1120\text{ (w, NA)}\text{ cm}^{-1}$, $1211\text{ (s, Tyr, Phe)}\text{ cm}^{-1}$, $1256\text{ (w, lipid)}\text{ cm}^{-1}$, $1303\text{ (w, protein+lipid)}\text{ cm}^{-1}$, $1330\text{ (s, phospholipid)}\text{ cm}^{-1}$, $1378\text{ (w, lipid)}\text{ cm}^{-1}$, $1440\text{ (w, lipids)}\text{ cm}^{-1}$, $1466\text{ (w, lipids)}\text{ cm}^{-1}$, $1552\text{ (w, Trp)}\text{ cm}^{-1}$, and $1600\text{ (w, Phe)}\text{ cm}^{-1}$. Also, there are some of the purification method-specific Raman peaks observed in the spectra including UC purified exosome specific peaks of 786 cm^{-1} , 852 cm^{-1} , 879 cm^{-1} , and 937 cm^{-1} or TEIR purified exosome specific peaks of 1175 cm^{-1} and 1394 cm^{-1} . All the assigned peaks are summarized in Table 1.

Table 1. Summary of Raman peaks from exosomes purified by TEIR and UC methods (s: strong, m: medium and w: weak)

Peak position (cm^{-1})	TEIR	UC	Origin	Ref.
615	s	s	C-C twisting protein	35
645	w	w	C-C twisting Tyr	36
707	w	s	aminoacid	37
752		s	nucleic acid	38
760	m		Trp	36
786		m	nucleic acid	39
830	m	w	Tyr	37
852		w	Tyr	35
879		w	Trp	40
920	s	w	protein	39
937		w	protein	40
1000	s	s	Phe	41
1050	m	m	lipid	42
1120	w	w	nucleic acid	42
1175	m		Tyr, Phe	35
1211	s	s	Tyr, Phe	43
1256		w	lipid	42
1303		w	protein+lipid	44
1330	s	s	phospholipid	41
1378		w	lipid	45
1394	s		CH rocking	46
1440	s	w	lipid	47
1466		w	lipid	42
1552	w	w	Trp	48
1600	w	w	Phe	48

We believe the discrepancy in SERS peaks between the two sets of exosomes mainly result from the exosome specific selectivity of the TEIR kit. Thus, the UC purified sample represents a broader population of exosomes, and possibly other similarly sized nanovesicles not necessarily originating from MVBs.

The specificity provided by the TEIR kit would selectively purify exosomes of certain kind while the ultra-centrifuged exosome may contain broader population distribution of exosomes and other impurities of exosome-sized microvesicles and debris secreted from

the cell, something also supported by size distribution of the exosome samples presented in Figure 1B. Here too, the UC sample is more varied in size, while the TEIR sample is fairly uniform in size. Furthermore, while the number of SERS peaks increases for the ultracentrifuged exosomes, so too does the spot to spot variation for a single UC-exosome nanobowl sample. The inconsistency between the SERS measurements of UC purified exosomes is represented by significantly larger standard deviation (Figure 5, grey lines) comparing to SERS of TEIR purified exosomes (Figure 4). PCA analysis showed mostly overlapped distribution, with only a limited separation between the two different time sets of SERS spectra for UC exosomes (Figure 5C). The samples were measured up to 24 hours and there was no significant change in peak positions after the 3 hr time point.

Conclusions

Exosomes derived from SKOV3 cell line were captured and analyzed inside nanobowls fabricated by soft lithography on PDMS substrates. Capturing of exosomes occurs when the solution containing the exosomes dries to the top of the nanobowls. The exosomes inside the bowls are still intact at this point, but will slowly burst as the solution inside the bowls completely dries out. When the exosomes are still intact, the majority of the observed SERS peaks are typical for the solution kit used for exosome isolation, indicating that molecules from the kit wrap around the surface of exosomes to aid in the separation process. SERS peaks typical for exosomes can be recovered by subtracting the signal originating from the exosome isolation kit. Due to the nature of the electric field enhancement in the SERS process, we attribute these peaks primarily to molecules in the vicinity of the SERS substrate, at or near the membrane of the exosomes. As the exosomes inside the bowl burst during the drying process, changes in the SERS spectra are observed. These changes can be attributed to the fact that, as the exosomes dry, they burst and release their molecular content, which can now be in close proximity to the SERS substrate and experience enhancement of the Raman signal. PCA of spectra recorded at different time points during the drying process further supports this hypothesis. SERS spectra from UC purified exosomes are also recorded and compared with the TEIR purified exosomes to provide additional support to the method.

We have shown that nanobowl-structured SERS substrates can capture and allow measurements for molecular-level characterization of nanometer-sized biological vesicles such as exosomes. This system can be used as a platform for disease diagnostics and the study the biological functions of exosomes.

Acknowledgements

This work was in part supported by NSF through NSF grant #1068109. We would like to thank Dr. Matt Mellema of the UC Davis School of Veterinary Medicine for running NTA of the samples and assisting in data analysis/interpretation. R.P.C. would like to acknowledge financial support from the T32 HL07013 training grant via the NIGH/NHLBI Training Program in Comparative Lung Biology and Medicine. We would also like to thank Dr. Ian Kennedy of UC Davis for giving us access to the COMSOL Multiphysics software.

Notes and references

¹Center for Biophotonics, University of California, Davis, Sacramento, CA 95817, USA

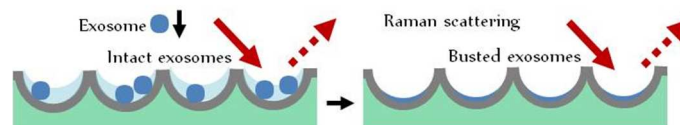
²Department of Biochemistry and Molecular Medicine, University of California, Davis, Sacramento, CA 95817, USA

³Department of Pathology and Laboratory Medicine, University of California, Davis, Sacramento, CA 95817, USA

*Email address: swachsmann@ucdavis.edu

1. C. Thery, L. Zitvogel and S. Amigorena, *Nature Reviews Immunology*, 2002, **2**, 569-579.
2. P. Vinciguerra and F. Stutz, *Current Opinion in Cell Biology*, 2004, **16**, 285-292.
3. D. J. Gibbings, C. Ciaudo, M. Erhardt and O. Voinnet, *Nature Cell Biology*, 2009, **11**, 1143-1149.
4. C. Grange, M. Tapparo, F. Collino, L. Vitillo, C. Damasco, M. C. Deregibus, C. Tetta, B. Bussolati and G. Camussi, *Cancer Research*, 2011, **71**, 5346-5356.
5. S. Rana, K. Malinowska and M. Zoller, *Neoplasia* 2013, **15**, 281-295.
6. S. Kim, N. Bianco, R. Menon, E. R. Lechman, W. J. Shufesky, A. E. Morelli and P. D. Robbins, *Molecular Therapy*, 2006, **13**, 289-300.
7. R. Valenti, V. Huber, M. Iero, P. Filipazzi, G. Parmiani and L. Rivoltini, *Cancer Research*, 2007, **67**, 2912-2915.
8. G. Rabinowitz, C. Gerel-Taylor, J. M. Day, D. D. Taylor and G. H. Kloecker, *Clinical Lung Cancer*, 2009, **10**, 42-46.
9. S. Sharma and J. J. Gimzewski, *Nanomedicine Nanotechnology*, 2012, **3**, 1000e115.
10. T. Katsuda, N. Kosaka and T. Ochiya, *Proteomics*, 2014, **14**, 412-425.
11. R. E. Lane, D. Korbie, W. Anderson, R. Vaidyanathan and M. Trau, *Scientific Report*, 2015, **5**.
12. D. S. Choi, D. K. Kim, Y. K. Kim and Y. S. Cho, *Proteomics*, 2013, **13**, 1554-1571.
13. C. Subra, K. Laulagnier, B. Perret and M. Record, *Biochimie*, 2007, **89**, 205-212.
14. R. J. Simpson, S. S. Jensen and J. W. E. Lim, *Proteomics*, 2008, **8**, 4083-4099.
15. E. Van Der Pol, A. G. Hoekstra, A. Sturk, C. Otto, T. G. Van Leeuwen and R. Nieuwland, *Journal of Thrombosis and Haemostasis*, 2010, **8**, 2596-2607.
16. Q. Zhang, Y. Li and R. W. Tsien, *Science*, 2009, **323**, 1448-1453.
17. K. Starchev, J. Buffle and E. Perez, *Journal of Colloid and Interface Science*, 1999, **213**, 479-487.
18. B. Hein, K. I. Willig and S. W. Hell, *Proceedings of the National Academy of Sciences*, 2008, **105**, 14271-14276.
19. S. Sahoo, E. Klychko, T. Thorne, S. Misener, K. M. Schultz, M. Millay, A. Ito, T. Liu, C. Kamide, H. Agrawal, H. Perlman, G. Qin, R. Kishore and D. W. Losordo, *Circulation Research*, 2011, **109**, 724-728.
20. V. Sokolova, A. K. Ludwig, S. Hornung, O. Rotan, P. A. Horn, M. Epple and B. Giebel, *Colloids and Surfaces B: Biointerfaces*, 2011, **87**, 146-150.
21. C. Admyre, S. M. Johansson, K. R. Qazi, J. J. Filin, R. Lahesmaa, M. Norman, E. P. A. Neve, A. Scheynius and S. Gabriellson, *The Journal of Immunology*, 2007, **179**, 1969-1978.
22. I. Tatischeff, E. Larquet, J. M. Falcon-Perez, P. Y. Turpin and S. G. Kruglik, *Journal of extracellular vesicles*, 2012, **1**, 19179.
23. L. T. Kerr, L. Gubbins, K. W. Gorzel, S. Sharma, M. Kell, A. Mc Cann and B. M. Hennelly, In *SPIE Photonics Europe*; International Society for Optics and Photonics: 2014, p 91292Q-91292Q-9.
24. M. Kahraman, P. Daggumati, O. Kurtulus, E. Seker and S. Wachsmann-Hogiu, *Scientific Reports*, 2013, **3**, 3396.
25. S. Jang, D. Choi, C. Heo, S. Lee and S. Yang, *Advanced Materials*, 2008, **20**, 4862-4867.
26. Z. Chen, T. Gang, X. Yan, J. Zhang, Y. Wang, X. Chen, Z. Sun, K. Zhang, B. Zhao and B. Yang, *Advanced Materials*, 2006, **18**, 924-929.
27. Y. Shen, M. Liu, Q. Wang, P. Zhan, Z. Wang, Q. Zhu, X. Chen, S. Jiang, X. Wang and C. Jin, *Nanoscale*, 2012, **4**, 2255-2259.
28. C. Thery, S. Amigorena, G. Raposo and A. Clayton, In *Current Protocols in Cell Biology*; John Wiley & Sons, Inc., 2006.
29. M. Kahraman and S. Wachsmann-Hogiu, *Analytica Chimica Acta*, 2014, **856**, 74-81.
30. W. Cho, Y. Kim and J. Kim, *ACS Nano*, 2012, **6**, 249-255.
31. K. Kreno, N. Greeneltch, O. Farha, J. Hupp and R. Van Duynem, *Analyst*, 2014, **139**, 4073-4080.
32. A. Marmur, *Langmuir*, 2003, **19**, 8343-8348.
33. H. Im, H. Shao, Y. Park, V. Peterson, C. Castro, R. Weissleder and H. Lee, *Nature Biotechnology*, 2014, **32**, 490-495.
34. L. Tirinato, F. Gentile, D. Di Mascolo, M. L. Coluccio, G. Das, C. Liberale, S. Pullano, G. Perozziello, M. Francardi, A. Accardo, F. De Angelis, P. Candeloro and E. Di Fabrizio, *Microelectronic Engineering*, 2012, **97**, 337-340.
35. J. Chan, D. Taylor, T. Zwerdling, S. Lane, K. Ihara and T. Huser, *Biophysical Journal*, 2006, **90**, 648-656.
36. I. Notingher, S. Verrier, S. Haque, J. Polak and L. Hench, *Biopolymers*, 2003, **72**, 230-240.
37. G. Shetty, C. Kedall, N. Shepherd, N. Stone and H. Barr, *British Journal of Cancer*, 2006, **94**, 1460-1464.
38. J. Bino, J. Abraham, I. Joe, V. Jayakumar, G. Petit and O. Nielsen, *Journal of Raman Spectroscopy*, 2004, **35**, 121-127.
39. N. Stone, C. Kendall, J. Smith, P. Crow and H. Barr, *Faraday Discussion*, 2004, **126**, 141-157.
40. W. Cheng, M. Liu, H. Liu and S. Lin, *Microscopy Research and Technique*, 2005, **68**, 75-79.
41. R. Malini, K. Venkatakrishna and J. Kurien, *Biopolymers*, 2006, **81**, 179-193.
42. R. Dukor, *Biomedical Applications*, 2002, **5**, 3335-3359.
43. D. Lau, Z. Huang, H. Lui and S. Qing, *Lasers in Surgery and Medicine*, 2005, **37**, 192-200.
44. Z. Huang, A. McWilliams, S. Lam, J. Englisg, D. McLean, H. Lui and H. Zeng, *International Journal of Oncology*, 2003, **23**, 649-655.
45. E. Kateinen, M. Elomaa, U. Laakkonen, E. Sippola, P. Niemela, J. Suhonen and K. Jaminen, *Journal of Forensic Science*, 2007, **52**, 88-92.
46. H. Schulz and M. Baranska, *Vibrational Spectroscopy*, 2007, **43**, 13-25.
47. R. Lakshmi, V. Kartha, C. Krishna, J. Solomon, G. Ullas and P. Uma Devi, *Radiation Research*, 2002, **157**, 175-182.
48. Z. Huang, A. McWilliams, M. Lui, D. McLean, S. Lam and H. Zeng, *International Journal of Cancer*, 2003, **107**, 1047-1052

Table of Contents



Nanobowl substrates are used to capture exosomes for SERS measurement which can provide biochemical analysis of intact and ruptured exosomes.